Materials Research Proceedings 28 (2023) 1443-1452 https://doi.org/10.21741/9781644902479-156

Micromechanical modeling of failure in dual phase steels

AYDINER Ilbilge Umay[1,a], TATLI Berkehan[1,b] and YALÇINKAYA Tuncay [1,c *]

[1]Department of Aerospace Engineering, Middle East Technical University, 06800, Ankara, Turkey

[a]aydiner.umay@metu.edu.tr, [b]btatli@metu.edu.tr, [c]yalcinka@metu.edu.tr

Keywords: Dual-Phase Steel, Cohesive Zone Modelling, Crystal Plasticity

Abstract. Having brittle martensitic islands diffused in a ductile ferrite matrix, dual-phase (DP) steels are known for their high formability and favorable material properties. Although they have already proven their advantages in the industry, there are still discussions regarding their microstructure-macroscopic response link. In order to effectively exploit their advantages and analyze their ductility in metal forming operations, the failure mechanisms of DP steels must be well examined following a micromechanics-based approach. There are a number of failure mechanisms to be addressed at the micro scale such as ferrite-martensite and ferrite-ferrite interface decohesion as well as martensite cracking depending on the different microstructural parameters and stress state. A crystal plasticity based finite element framework for RVE calculations is followed here based on the previous work which focuses solely on the plastic deformation (see [1]). Isotropic J2 plasticity model is employed for the hard martensite phase while the rate-dependent crystal plasticity framework is used for the ductile ferrite phase. Cohesive zone elements are inserted at the ferrite-martensite and ferrite-ferrite interfaces for intergranular cracking analysis, besides, intragranular cracking in martensite phase is addressed through an uncoupled damage model. First, a preliminary study was performed in order to identify and calibrate aforementioned failure models, then, various 3D polycrystalline RVEs having different microstructural parameters loaded with different stress triaxialities are analyzed and discussed adding up to the preliminary discussions presented in [2].

Introduction

Dual-phase (DP) steels are one of the material groups most favored by the automotive industry due to their good formability without compromising on high strength. These mechanically advantageous characteristics of dual phase steels stem from the micromechanical cooperation between two different phases, namely the soft ferrite phase and the hard martensite phase. Martensite islands are interspersed between the ferrite grains and this heterogeneous microstructure translates to complex fracture mechanisms that should be studied in the micro scale. Stress concentration and strain localization due to the strength and ductility contrast between two constituent phases lead to various failure mechanisms. Although previous works give various results about the exact location of the failure initiation, three different types of damage nucleation modes have been identified to predominate in DP steels which are ferrite/ferrite (F/F) decohesion, ferrite/martensite (F/M) decohesion and martensite cracking (see [3-6]). Therefore, each failure mechanism should be analyzed with a separate compatible technique and a multiscale approach is essential to establish the macroscale results of plastic deformation, damage evolution and crack initiation occurring at the microscale. The variation of dominant damage nucleation mode is mainly dependent on martensite distribution and volumetric fraction [3,4,6]. Still, according to [7] failure in DP-steels is highly related also with the stress state, and one should place greater emphasis on the effect of triaxiality variation on the material. Most of the previous works [8,9] have been centered around uniaxial tension cases, yet there exist few papers mentioning different stress states [10]. There are examples of modeling DP in either simplified or realistic dual phase

microstructures (see e.g. [8-12]) at representative volume element (RVE) scale. Due to its low ductility, phenomenological models are deemed sufficient to represent the constitutive behavior of martensite phase while ferrite deformation is handled by both phenomenological and crystal plasticity models (see e.g. [1,12]). For the modelling of void nucleation and growth among ferrite grains, Modified Mohr-Coulomb (MMC) [10] and Gurson-Tvergaard-Needleman (GTN) [13,14] models are used in the literature. Martensite cracking on the other hand, has been modeled with various approaches such as the extended finite element method (XFEM) [14], maximum principal stress criterion [10] and Bao-Wierzbicki failure criterion [15]. Ferrite/ferrite [13] and ferrite/martensite [9,11,16] grain boundary decohesion have been observed by the incorporation of cohesive zone model (CZM). Parameter identification of cohesive elements has been performed through nanoindentation tests [16] and compact tension (CT) specimen simulations [13] by obtaining critical failure stress and fracture energy.

In this study, three dimensional RVEs are generated using Voronoi tessellations where J_2 plasticity and crystal plasticity frameworks are employed for the martensite and ferrite phases respectively. The main goal is to predict crack initiation and progression in DP steel by inserting cohesive elements to model the decohesion of ferrite/ferrite and ferrite/martensite interfaces. Moreover, an uncoupled damage model is employed in order to model the intragranular cracking of martensite phase. Each type of decohesion is simulated with a different set of interface parameters to obtain the appropriate constitutive behavior. Both the experimental results from the literature and the numerical techniques are used for parameter identification. Those numerical techniques include an inclusion RVE study, CT specimen and nanoindentation simulations. Crystal plasticity parameters are also obtained through an RVE study of pure ferrite phase. Lastly, polycrystalline dual phase RVEs are analyzed under various stress states, martensite distributions and crystallographic orientations to discuss and compare the failure results with respect to the observations in the literature.

Constitutive Models

Ferrite phase is modeled with rate dependent crystal plasticity framework that links the crystallographic slip at the microscale to the macroscopic deformation measures. In this framework, the two fundamental mechanisms causing the macroscopic deformation are elastic lattice distortion and crystallographic slip caused by dislocation motion on active slip systems (see [17,18]). The deformation gradient is multiplicatively divided into an elastic and a plastic part in the finite strain formulation that serves as the basis for the crystal plasticity model employed here,

$$\mathbf{F}=\mathbf{F}_e\cdot\mathbf{F}_p \tag{1}$$

The rate of change of $\mathbf{F}_p$ is related to the plastic slip rates $\dot{\gamma}^\alpha$ of the α by,

$$\dot{\mathbf{F}}_p\cdot\mathbf{F}_p^{-1}=\sum_\alpha \dot{\gamma}^\alpha \mathbf{m}^\alpha\otimes\mathbf{n}^\alpha, \tag{2}$$

where $\mathbf{m}^\alpha$ and $\mathbf{n}^\alpha$ represent the slip direction and slip normal in the reference configuration. Power law relation is used to obtain the evolution of plastic slip rate $\dot{\gamma}^\alpha$,

$$\dot{\gamma}^\alpha=\dot{\gamma}_0\left|\frac{\tau^\alpha}{g^\alpha}\right|^n \mathrm{sign}(\tau^\alpha) \tag{3}$$

where $\dot{\gamma}_0$ refers to the reference plastic slip rate and n refers to the rate sensitivity exponent. τ^α denotes the resolved shear stress and g^α is the slip resistance on the slip system α that controls the hardening of the single crystal. Evolution of slip resistance is governed by,

$$\dot{g}^{\alpha}=\sum_{\beta} h^{\alpha\beta}\left|\dot{\gamma}^{\beta}\right| \tag{4}$$

where $h^{\alpha\beta}$ and $h^{\alpha\alpha}$ denotes the latent hardening matrix and self-hardening rate respectively. Following basic forms are adapted for the evolution of those,

$$h^{\alpha\alpha}=h_0 \operatorname{sech}^2\left|\frac{h_0\gamma}{g_s-g_0}\right| \tag{5}$$

$$h^{\alpha\beta}=q^{\alpha\beta}h^{\alpha\alpha} \quad (\alpha\neq\beta) \tag{6}$$

where h_0 is the initial hardening modulus, g_0 is the initial slip resistance and g_s is the saturation slip resistance. Crystal plasticity simulations of the ferrite phase in this paper use {112}[111] slip family.

Due to the very limited ductile deformation, the martensite phase is modeled with J_2 plasticity framework with isotropic hardening in order to have a less expensive analysis, while ferrite phase, which accommodates the majority of the deformation in DP steels is simulated through a crystal plasticity model. The martensite plasticity model is described as [19],

$$\sigma_{y,m}=\sigma_{y_0,m}+k_m\left(1-\exp\left(-\varepsilon_p n_m\right)\right) \tag{7}$$

$$\sigma_{y_0,m}=300+1000C_m^{1/3} \tag{8}$$

$$k_m=\frac{1}{n_m}\left[a+\frac{bC_m}{1+\left(\frac{C_m}{C_0}\right)^q}\right] \tag{9}$$

where $\sigma_{y,m}$, ε_p and C_m denotes respectively the current yield strength, accumulated plastic strain and carbon content expressed in wt.%. Initial yield stress, $\sigma_{y_0,m}$, hardening modulus, k_m and hardening exponent, n_m, are material parameters. The values provided by [19] are used for the hardening parameters of the martensite phase throughout this study and given as, C_m=0.3 wt%, a=33 GPa, C_0=0.7, q=1.45, b=360 GPa, n_m=120. Moreover, the Young's modulus and Poisson's ratio are taken to be E=210 GPa and ν=0.3, respectively.

Failure Models

Bao and Wierzbicki failure criterion [20] is adopted to predict the intragranular failure in martensite grains. In this criterion, equivalent plastic strain to fracture $\bar{\varepsilon}_f$ is assumed to be dependent on the stress triaxiality $\eta=\sigma_m/\bar{\sigma}$, in which $\bar{\sigma}$ is the Von Mises equivalent stress and σ_m is the mean stress. The fracture locus can be accurately characterized by a piece-wise function of the following form when stress triaxiality is assumed to be constant throughout the experiment,

$$\bar{\varepsilon}_f=\begin{cases}\dfrac{C_1}{1+3\eta}, & -1/3\leq\eta\leq 0\\ C_2+(C_2-C_1)(3\eta-1), & 0\leq\eta\leq 1/3\\ C_2\exp\left(-\alpha(\eta-1/3)\right), & \eta\geq 1/3\end{cases} \tag{10}$$

where $C_1=\bar{\varepsilon}_f^{ss}$ is the equivalent plastic strain to fracture in pure shear, $C_2=\bar{\varepsilon}_f^{UT}$ is the equivalent plastic strain to fracture in uniaxial tension and α is the fitting parameter used for large triaxiality values. Damage accumulation is calculated by considering the following integral,

$$D(\bar{\varepsilon}_p) = \int_0^{\bar{\varepsilon}_p} \frac{1}{\bar{\varepsilon}_f} d\bar{\varepsilon}_p \tag{11}$$

It follows that, damage only increases as $\bar{\varepsilon}_f$ is always positive according to Eq. 10.

The Park-Paulino-Roesler (PPR) model [21], a unified, mixed-mode, potential based cohesive zone model, is used to simulate the decohesion of the ferrite/ferrite and ferrite/martensite grain boundaries. The framework has already been applied successfully for the intergranular cracking in polycrystalline plasticity (see [22]). The following is a definition of the potential function of PPR,

$$\psi(\Delta_n,\Delta_t)= \min(\phi_n,\phi_t) + \left[\Gamma_n \left(1-\frac{\Delta_n}{\delta_n}\right)^{\alpha} \left(\frac{m}{\alpha}+\frac{\Delta_n}{\delta_n}\right)^{m} +\phi_n-\phi_t\right] \times \left[\Gamma_t \left(1-\frac{|\Delta_t|}{\delta_t}\right)^{\beta} \left(\frac{n}{\beta}-\frac{|\Delta_t|}{\delta_t}\right)^{n} +\phi_t-\phi_n\right] \tag{12}$$

Here, m, n are non-dimensional exponents, α, β are shape parameters, δ_n, δ_t are the normal and tangential final crack opening widths, ϕ_n, ϕ_t are fracture energies in normal and tangential directions, Δ_n is the normal separation, Δ_t is the effective sliding displacement. Γ_n, Γ_t are energy constants that are related to shape parameters and initial slope indicators. Shape parameters α, β define the softening responses and λ_n, λ_t are the initial slope indicators that control cohesive stiffness and cohesive elastic behavior. Fracture energies ϕ_n, ϕ_t are the areas under the pure normal and tangential traction–separation curves. The traction functions are defined as the derivatives of the potential function with respect to corresponding separations,

$$T_n(\Delta_n,\Delta_t)= \frac{\partial \psi}{\partial \Delta_n}, \; T_t(\Delta_n,\Delta_t)= \frac{\partial \psi}{\partial \Delta_t} \tag{13}$$

When separation reaches critical values, the traction is equal to the corresponding cohesive strength (σ_{max}, τ_{max}). Nine input parameters, including normal fracture energy (ϕ_n), tangential fracture energy (ϕ_t), normal cohesive strength (σ_{max}), tangential cohesive strength (τ_{max}), normal shape parameter (α), tangential shape parameter (β), normal initial slope indicator (λ_n), and tangential initial slope indicator (λ_t) are needed to be identified to model the behavior of each interface. For more details about the formulation and applications see [2,23].

The ability of the model to capture the mixed mode fracture makes it very suitable to three-dimensional framework of this study.

Numerical Implementation

Material parameters of ferrite phase are identified through a generated pure ferrite polycrystalline RVE. Cubic elastic parameters are taken from [24] as C_{11}=231.4 GPa, C_{12}=134.7 GPa, C_{44}=116.4 GPa and experimental data presented in [6] is utilized to fit the flow curves obtained from RVE simulations (see [12] for more details). Obtained hardening parameters are tabulated in Table 1. Reference slip rate $\dot{\gamma}_0$ is taken to be 0.001 s^{-1} while rate sensitivity exponent n is determined as 25 and the ratio of latent to self-hardening assumed to be 1.

Table 1. Crystal plasticity parameters for ferrite phase.

Slip Systems	g_s [MPa]	h_0 [MPa]	g_0 [MPa]
{112}⟨111⟩	252	475	98

Eq. 1-6 with the provided material parameters are implemented as a user material subroutine (UMAT) in ABAQUS software based on the framework of Huang (see [25]).

Bao-Wierzbicki uncoupled damage model (see Eq. 3) is applied amongst martensite grains to observe the damage behavior of martensite phase in polycrystal RVEs. The parameter identification of the model is performed by the simulation of a tensile specimen to match the

experimental data of the martensite phase given in [6] (see e.g. [15]). Obtained model parameters are α=1.54, C_1=0.04 and C_2=0.04. This damage model with the provided model parameters is then implemented in ABAQUS by means of a user-defined field subroutine (USDFLD).

Identification of PPR cohesive zone model parameters is a rather comprehensive problem. Since ferrite/ferrite grain boundary decohesion is also considered on top of ferrite/martensite grain boundary decohesion in this study, PPR model parameters of both interfaces must be fitted all together to the experiments. For that, first results provided in [2] are utilized for ferrite/martensite interface. Then, in order to find the critical stress and failure energy of the ferrite/ferrite interface a CT-specimen study is performed as exemplified in [13]. Lastly, ferrite/martensite inclusion problem that includes both ferrite/ferrite and ferrite/martensite interfaces is analyzed for the final parameter calibration of each constituent interface simultaneously. For compactness, details of the parameter identification study for PPR cohesive zone model are not shown here. See Table 2 for the identified model parameters for the ferrite/ferrite and ferrite/martensite interfaces.

Table 2. Calibrated PPR CZM parametes for ferrite/ferrite and ferrite/martensite interfaces.

Interface	σ_{max} [MPa]	τ_{max} [MPa]	ϕ_n [N/mm]	ϕ_t[N/mm]	α	β	λ_n	λ_t
F/F	650	227.5	230	230	4.46	2.74	0.001	0.002
F/M	1500	525	0.4	0.4	4.46	2.74	0.01	0.02

In the FE calculations, 10-node second-order tetrahedral elements (C3D10) are used to simulate bulk elements, while 12-node compatible triangular cohesive elements are used between the interfaces. The Voronoi-based tessellation generator software Neper [26] was used to create 3D microstructures. Input files are modified by an in-house MATLAB code that identifies the ferrite/ferrite and ferrite/martensite interfaces and inserts cohesive elements to those interfaces by considering element connectivity in the original mesh. Updated input files are then run through ABAQUS along with the user material subroutines (UMAT) for both crystal and J2 plasticity, user element subroutine (UEL) for the PPR CZM and user-defined field (USDFLD) for the Bao-Wierzbicki damage model. The next section presents and discusses the findings.

Numerical Examples

This section presents numerical findings in three-dimensional RVEs, and briefly discusses the impact of microstructural parameters on the plastic deformation and failure behavior of dual-phase steels. This is accomplished by producing a number of cubic polycrystalline RVEs, which are non-periodic, with 250 and 280 randomly oriented and distributed grains. There are two main morphologies with different martensite distributions but same volumetric fraction of 15%. The input files for ABAQUS are generated via an in-house MATLAB script as mentioned previously. While the martensite phase is assigned to the classical J_2 plasticity theory with isotropic hardening as given in Eq. 7, the rate-dependent crystal plasticity model that has been presented through Eq. 1–6 with the hardening parameters in Table 1 is assigned to the ferrite phase. Boundary conditions are defined such that RVE analysis can follow the mechanical response of the material under various stress states that have different overall triaxiality values (see [12] for more details). For all simulations, applied strain rate is assumed to be 0.001 s^{-1}. Volumetric averaging method is then used to obtain the true stress-strain curves.

First, six RVEs, each of three having the same martensite distribution, are analyzed. Crystal orientations of ferrite grains are randomly changed for each RVE to study the effect of grain orientation and microstructure on the material response and damage initiation. Fig. 1 shows the homogenized stress-strain curves of the simulations plotted on top of the experimental results [6].

The results from the first morphology show a slight anisotropy due to the relatively lower number of ferrite grains with respect to the second morphology. When Fig. 1a is compared to Fig. 1b, it is very obvious that variation in the martensite distribution and morphology changes the overall response of the material to a great extent. Looking at this figure, the effect of crystal orientation may not be clear enough to distinguish. In order to have a better understanding of how grain orientation affects the stress and damage evolution on the microstructure, von Mises Stress and damage contours are plotted for each morphology at the same cross section and instant in Fig. 2 and Fig. 3. Here, by examining the significant difference between decohesion, deformation and damage accumulation patterns, one can easily deduce that microstructural parameters of DP-steels have a considerable influence on the crack initiation, growth, and propagation. Here, it should be noted that ferrite grains are colored gray in all damage distribution contours as no damage model is employed for the ferrite phase.

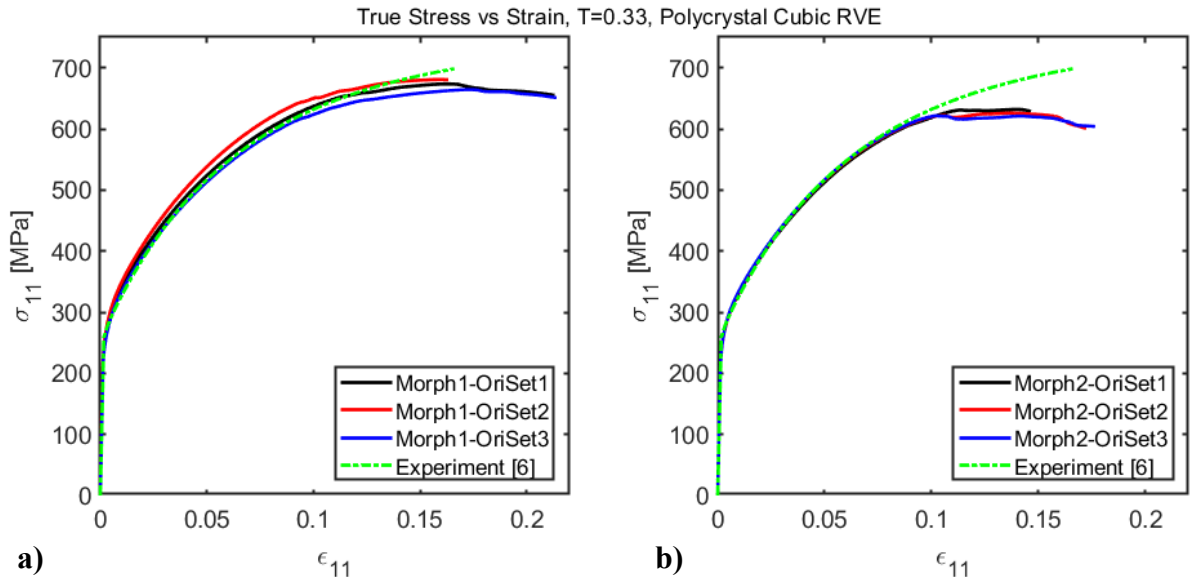

Fig. 1. True stress versus true strain curves of a) the first morphology b) the second morphology with three different orientation sets.

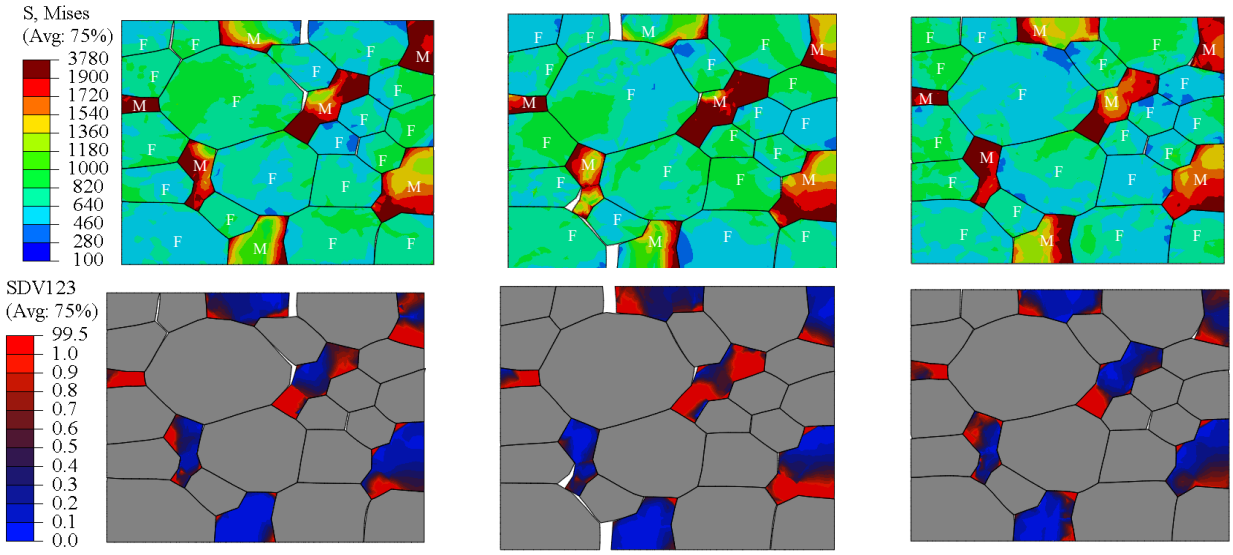

Fig. 2. Von Mises Stress (Top) and Damage (Bottom) distributions of Morph1-Oriset1 (Left), Morph1-Oriset2 (Middle), Morph1-Oriset3 (Right). F: Ferrite, M: Martensite.

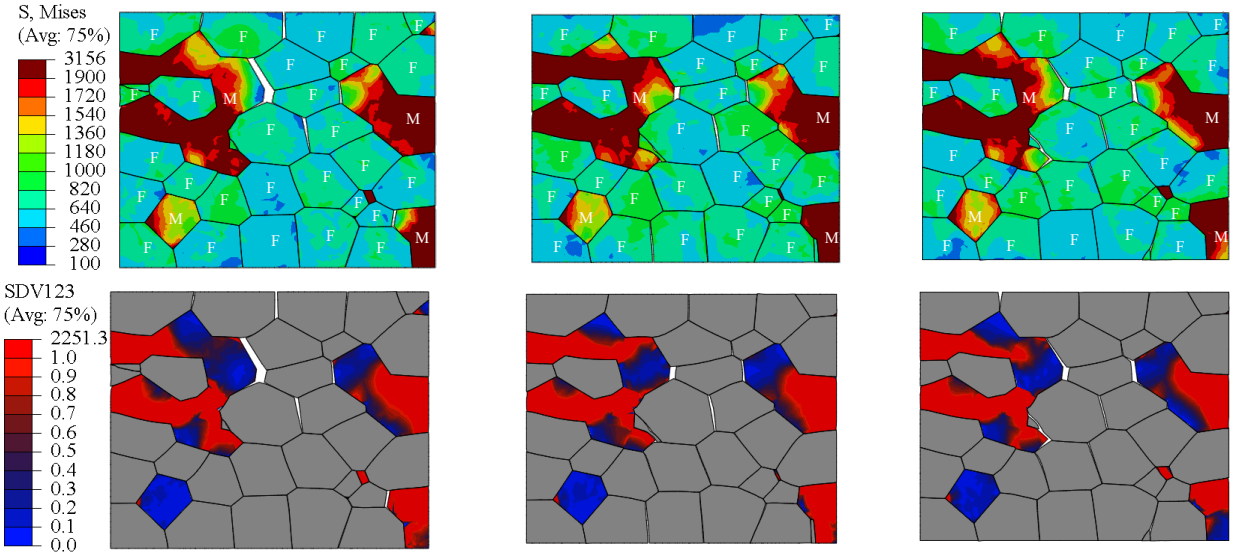

Fig. 3. Von Mises Stress (Top) and Damage (Bottom) distributions of Morph2-Oriset1 (Left), Morph2-Oriset2 (Middle), Morph2-Oriset3 (Right). F: Ferrite, M: Martensite.

Then, the analyses are carried out for three RVEs having the same crystal orientation and martensite distribution with three different stress triaxialities. Martensite distribution selected here is the same as the first morphology to be able to capture the sole effect of stress state on the failure mechanisms and stress distribution. Obtained flow curves are shown in Fig. 4. As per expectations, higher stress triaxiality translates to lower failure strains. From Fig. 5, it can be inferred that when triaxiality is held at 1.5, intergranular decohesion leads to complete failure with the martensite grains remaining below critical damage, in contrast with the other examples.

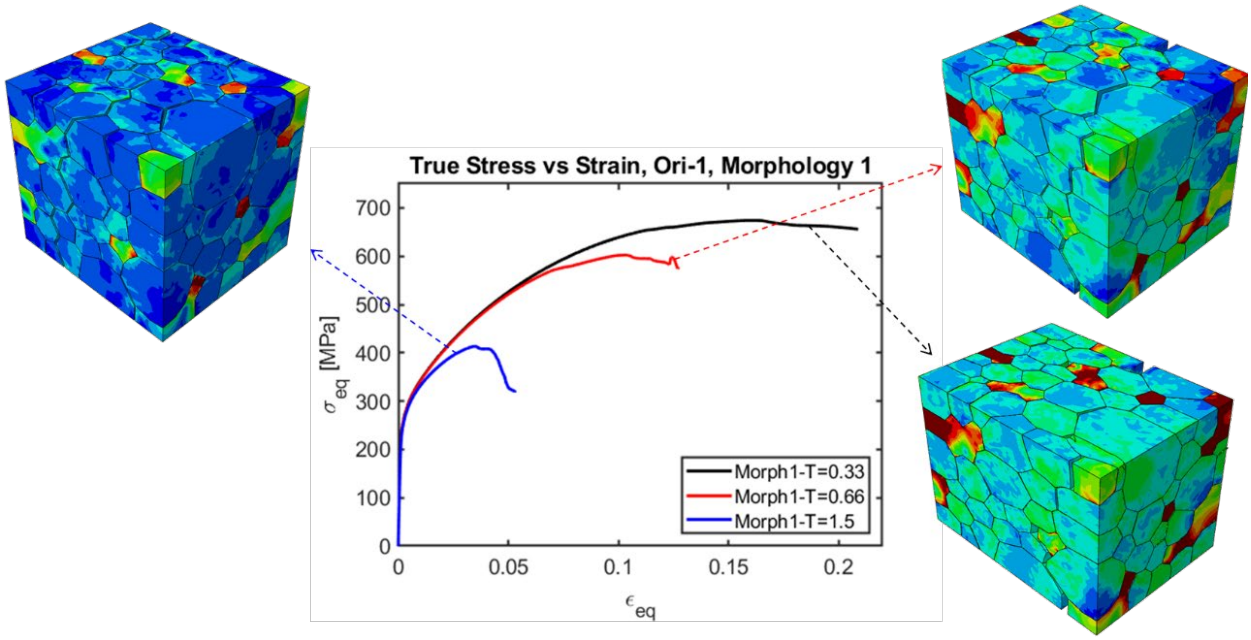

Fig. 4. True stress versus true strain curves of the first morphology with three different stress triaxialities.

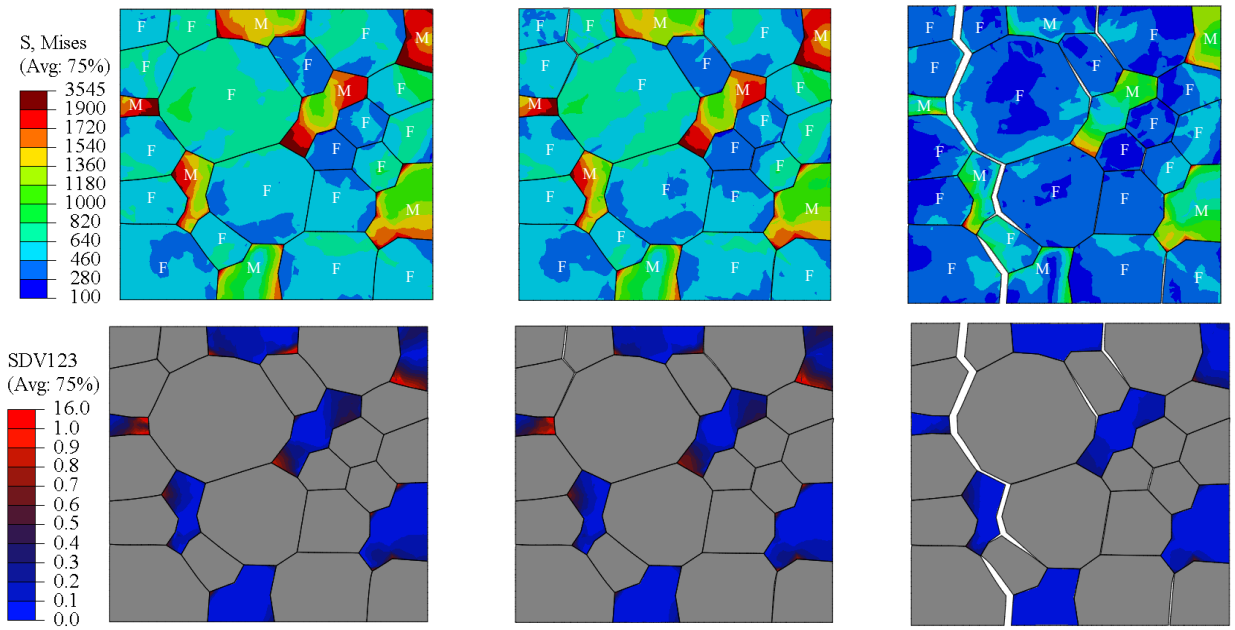

Fig. 5. Von Mises Stress (Top) and Damage (Bottom) distributions of Morph1-T=0.33 (Left), Morph1-T=0.66 (Middle), Morph1-T=1.5 (Right). F: Ferrite, M: Martensite.

Summary

This study makes an attempt to address the microstructure evolution, constitutive response, and failure in three-dimensional dual phase steel microstructures through polycrystalline RVEs employing J_2 and crystal plasticity frameworks in addition to cohesive zone and damage models. Analyses are performed for different orientation sets and morphologies under various stress triaxialities. The study clearly demonstrates how damage and fracture behavior of DP steels at the microstructure scale depend on the orientation set, morphology, and triaxiality. Obtained results prove that for the numerical analysis of failure in DP-steels, an extensive study in microscale is

necessary that includes modeling of inter/intra-granular failure mechanisms, and microstructural evolution.

References

[1] T. Yalçinkaya, S.O. Çakmak, C. Tekoglu, A crystal plasticity based finite element framework for RVE calculations of two-phase materials: Void nucleation in dual-phase steels, Finite Elem. Anal. Des. 187 (2021) 103510. https://doi.org/10.1016/j.finel.2020.103510
[2] T. Yalçinkaya, B. Tatli, I.E. Ünsal, I.U. Aydiner, Crack Initiation and Propagation in Dual-phase Steels Through Crystal Plasticity and Cohesive Zone Frameworks, Procedia Struct. Integrity 42 (2022) 1651-1659. https://doi.org/10.1016/j.prostr.2022.12.208
[3] J. Kadkhodapour, A. Butz, S. Ziaei Rad, Mechanisms of void formation during tensile testing in a commercial, dual-phase steel, Acta Mater. 59 (2011) 2575-2588. https://doi.org/10.1016/j.actamat.2010.12.039
[4] A. Tang, H. Liu, R. Chen, G. Liu, Q. Lai, Y. Zhong, L. Wang, J. Wang, Q. Lu, Y. Shen, Mesoscopic origin of damage nucleation in dual-phase steels, Int. J. Plast. 137 (2021) 102920. https://doi.org/10.1016/j.ijplas.2020.102920
[5] G. Avramovic-Cingara, Y. Ososkov, M.K. Jain, D.S. Wilkinson, Effect of martensite distribution on damage behaviour in DP600 dual phase steels, Mater. Sci. Eng., A 516 (2009) 7-16. https://doi.org/10.1016/j.msea.2009.03.055
[6] Q. Lai, O. Bouaziz, M. Gouné, L. Brassart, M. Verdier, G. Parry, A. Perlade, Y. Bréchet, T. Pardoen, Damage and fracture of dual-phase steels: Influence of martensite volume fraction, Mater. Sci. Eng. A 646 (2015) 322-331. https://doi.org/10.1016/j.msea.2015.08.073
[7] S. Qin, R. McLendon, V. Oancea, A.M. Beese, Micromechanics of multiaxial plasticity of DP600: Experiments and microstructural deformation modeling, Mater. Sci. Eng. A 721 (2018) 168-178. https://doi.org/10.1016/j.msea.2018.02.078
[8] X. Sun, K.S. Choi, W.N. Liu, M.A. Khaleel, Predicting failure modes and ductility of dual phase steels using plastic strain localization, Int. J. Plast. 25 (2009) 1888-1909. https://doi.org/10.1016/j.ijplas.2008.12.012
[9] J. Kadkhodapour, B. Anbarlooie, H. Hosseini-Toudeshky, S. Schmauder, Simulation of shear failure in dual phase steels using localization criteria and experimental observation, Comput. Mater. Sci. 94 (2014) 106-113. https://doi.org/10.1016/j.commatsci.2014.02.046
[10] S. Qin, Y. Lu, S.B. Sinnott, A.M. Beese, Influence of phase and interface properties on the stress state dependent fracture initiation behavior in DP steels through computational modeling, Mater. Sci. Eng. A 776 (2020) 138981. https://doi.org/10.1016/j.msea.2020.138981
[11] H. Hosseini-Toudeshky, P. Parandavar, B. Anbarlooie, Stress–strain prediction of dual phase steels using 3D RVEs considering both interphase hardness variation and interface debonding at grain boundaries, Arch. Appl. Mech. 92 (2022) 255–270. https://doi.org/10.1007/s00419-021-02054-5
[12] T. Yalcinkaya, G.O. Gungor, S.O. Cakmak, C. Tekoglu, A micromechanics based numerical investigation of dual phase steels, Procedia Struct. Integrity 21 (2019) 61-72. https://doi.org/10.1016/j.prostr.2019.12.087
[13] V. Uthaisangsuk, U. Prahl, W. Bleck, Micromechanical modelling of damage behaviour of multiphase steels, Comput. Mater. Sci. 43 (2008) 27-35. https://doi.org/10.1016/j.commatsci.2007.07.035
[14] N. Vajragupta, V. Uthaisangsuk, B. Schmaling, S. Münstermann, A. Hartmaier, W. Bleck, A micromechanical damage simulation of dual phase steels using XFEM, Comput. Mater. Sci. 54 (2012) 271-279. https://doi.org/10.1016/j.commatsci.2011.10.035
[15] Matsuno, C. Teodosiu, D. Maeda, A. Uenishi, Mesoscale simulation of the early evolution of ductile fracture in dual-phase steels, Int. J. Plast. 74 (2015) 17-34. https://doi.org/10.1016/j.ijplas.2015.06.004

[16] H. Hosseini-Toudeshky, B. Anbarlooie, J. Kadkhodapour, Micromechanics stress–strain behavior prediction of dual phase steel considering plasticity and grain boundaries debonding, Mater. Des. 68 (2015) 167-176. http://doi.org/10.1016/j.matdes.2014.12.013
[17] T. Yalcinkaya, W.A.M. Brekelmans, M.G.D. Geers, BCC single crystal plasticity modeling and its experimental identification, Modell. Simul. Mater. Sci. Eng. 16 (2008) 085007. http://doi.org/10.1088/0965-0393/16/8/085007
[18] O. Bulut, S.S. Acar, T. Yalçinkaya, The influence of thickness/grain size ratio in microforming through crystal plasticity, Procedia Struct. Integrity 35 (2022) 228-236. https://doi.org/10.1016/j.prostr.2021.12.069
[19] A.P. Pierman, O. Bouaziz, T. Pardoen, P.J. Jacques, L. Brassart, The influence of microstructure and composition on the plastic behaviour of dual-phase steels, Acta Mater. 73 (2014) 298-311. https://doi.org/10.1016/j.actamat.2014.04.015
[20] Y. Bao, T. Wierzbicki, On fracture locus in the equivalent strain and stress triaxiality space, Int. J. Mech. Sci. 46 (2004) 81–98. https://doi.org/10.1016/j.ijmecsci.2004.02.006
[21] K. Park, G.H. Paulino, J.R. Roesler, A unified potential-based cohesive model of mixed-mode fracture, J. Mech. Phys. Solids 57 (2009) 891–908. https://doi.org/10.1016/j.jmps.2008.10.003
[22] T. Yalçinkaya, İ. Özdemir, A.O. Firat, Inter-granular cracking through strain gradient crystal plasticity and cohesive zone modeling approaches, Theor. Appl. Fract. Mech. 103 (2019) 102306. https://doi.org/10.1016/j.tafmec.2019.102306
[23] A. Cerrone, P. Wawrzynek, A. Nonn, G.H. Paulino, A. Ingraffea, Implementation and verification of the Park–Paulino–Roesler cohesive zone model in 3D, Eng. Fract. Mech. 120 (2014) 26-42. https://doi.org/10.1016/j.engfracmech.2014.03.010
[24] W. Woo, V.T. Em, E.-Y. Kim, S.H. Han, Y.S. Han, S.-H. Choi, Stress–strain relationship between ferrite and martensite in a dual-phase steel studied by in situ neutron diffraction and crystal plasticity theories, Acta Mater. 60 (2012) 6972-6981. https://doi.org/10.1016/j.actamat.2012.08.054
[25] Y. Huang, A User-Material Subroutine Incorporating Single Crystal Plasticity in the ABAQUS Finite Element Program, 1991.
[26] R. Quey, P.R. Dawson, F. Barbe, Large-scale 3D random polycrystals for the finite element method: Generation, meshing and remeshing, Comput. Methods Appl. Mech. Eng. 200 (2011) 1729-1745. https://doi.org/10.1016/j.cma.2011.01.002